

# Universality of the Kondo effect in quantum dots with ferromagnetic leads

M. Gaass,<sup>1,\*</sup> A. K. Hüttel,<sup>1</sup> K. Kang,<sup>1,2</sup> I. Weymann,<sup>3,4</sup> J. von Delft,<sup>3</sup> and Ch. Strunk<sup>1</sup>

<sup>1</sup>*Institute for Exp. and Applied Physics, University of Regensburg, 93040 Regensburg, Germany*

<sup>2</sup>*Department of Physics, Chonnam National University, Gwang-Ju 500-757, Korea*

<sup>3</sup>*Physics Department, ASC, and CeNS, Ludwig-Maximilians-Universität, 80333 Munich, Germany*

<sup>4</sup>*Department of Physics, Adam Mickiewicz University, 61-614 Poznań, Poland*

(Dated: October 29, 2018)

We investigate quantum dots in clean single-wall carbon nanotubes with ferromagnetic PdNi-leads in the Kondo regime. In most odd Coulomb valleys the Kondo resonance exhibits a pronounced splitting, which depends on the tunnel coupling to the leads and an external magnetic field  $B$ , and only weakly on gate voltage. Using numerical renormalization group calculations, we demonstrate that all salient features of the data can be understood using a simple model for the magnetic properties of the leads. The magnetoconductance at zero bias and low temperature depends in a universal way on  $g\mu_B(B - B_c)/k_B T_K$ , where  $T_K$  is the Kondo temperature and  $B_c$  the external field compensating the splitting.

PACS numbers: 73.23.Hk, 73.63.Fg, 72.15.Qm, 72.25.-b

The Kondo effect resulting from the exchange interaction of a single spin with a bath of conduction electrons [1], is one of the archetypical phenomena of many-body physics. Its competition with ferromagnetism and possible applications in spintronics [2] have raised wide interest in the past few years. The Kondo effect in quantum dots [3, 4] has, in recent experiments, been investigated in the presence of ferromagnetic (FM) leads [5–7]. It was found that the Kondo resonance, usually observed at zero bias in the odd Coulomb blockade (CB) valleys, is split into two peaks at finite bias [5]. The splitting consists of a term depending logarithmically on gate voltage [6, 7], and, as demonstrated here, a second term nearly independent of gate voltage. These phenomena were predicted theoretically [8–11], attributing the splitting of the Kondo resonance to a tunneling induced exchange field, which results from the magnetic polarization of the leads. So far no detailed and quantitative comparison of the measured conductance with the theory has been undertaken to verify whether the simplistic description of FM leads used in Refs. 8–11 has quantitative predictive power. The latter would be needed for future spintronics applications that exploit the lead-induced local spin splitting, e.g., spin filtering.

In this Letter we present low-temperature transport measurements of a single wall carbon nanotube quantum dot with PdNi leads. We concentrate on the less studied gate-independent contribution of the exchange splitting of the Kondo resonance and attribute it to the saturation magnetization of the contact material. We show that the evolution of the conductance with magnetic field and gate voltage can be understood within a simple model for the magnetization and polarization in the FM leads, by presenting numerical renormalization group (NRG) calculations for this model, using parameters extracted from experiment. Moreover, by comparing resonances of different transparency, we demonstrate a universal scaling

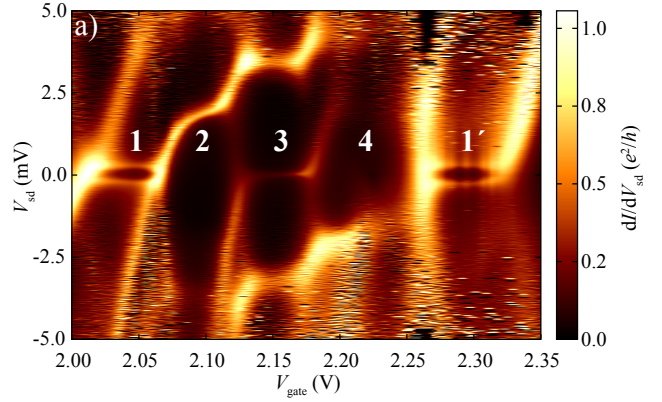


FIG. 1. (Color online) Differential conductance  $dI/dV_{sd}$  versus bias voltage  $V_{sd}$  and gate voltage  $V_{gate}$  at  $T = 25$  mK and  $B = 0$  T. The CB regions are numbered for future reference.

of the magnetic field dependence of the Kondo conductance, proving that the magnetization of the leads can indeed be viewed as an exchange field, which acts analogously to an external magnetic field.

*Experimental setup.*— The nanotubes are grown by chemical vapor deposition on a highly doped silicon substrate with a 200 nm thermally grown oxide layer at its surface [12]. The contact electrodes with a thickness of roughly 45 nm are subsequently structured by electron beam lithography and consist of  $\text{Pd}_{0.3}\text{Ni}_{0.7}$ , known to generate highly transparent contacts [13]. Transport measurements were done in a dilution refrigerator with a base temperature of 25 mK. The current  $I$  is measured in a two point geometry with a voltage bias  $V_{sd}$  applied to the source contact.

The differential conductance  $G = dI/dV_{sd}$  is plotted in Fig. 1 in color scale, providing the typical charging diagram of a quantum dot [14]. Our device exhibits regular CB oscillations and a clear fourfold symmetry characteristic for carbon nanotubes [15]. Coupling to the contacts is strong, leading to broad resonance lines and a variety

of higher-order processes. Fig. 1 implies the following parameters for the nanotube quantum dot [15, 16]: a charging energy  $U \simeq 5$  meV, a level separation  $\Delta \simeq 9.5$  meV, and a subband mismatch of about  $\delta \simeq 1$  meV. The tunnel coupling  $\Gamma$  between leads and quantum dot can be inferred from the line width of the conductance peak. Between valleys 1 and 2 in Fig. 1 we obtain a full width at half maximum (FWHM) of  $\Gamma = 1.1$  meV  $\gg k_B T$ .

A striking feature visible in Fig. 1 are lines of enhanced conductance at small, approximately constant bias values in every second CB diamond. We attribute these lines to a spin-1/2 Kondo conductance anomaly, split into two peaks at small opposite bias values due to the presence of FM contacts. The peak distance  $2\Delta\varepsilon$  at the center of the diamond can be related to a magnetic field scale  $B = \Delta\varepsilon/g\mu_B$  via the Zeeman effect. For valley 1 in Fig. 1 this gives approximately 2 T for  $g = 2$ . Some resonances with very low conductance exhibit no measurable splitting.

*Main features of  $B$ -dependence:*— Figure 2(a) displays detailed measurements of valley 1 from Fig. 1 for different values of external magnetic fields almost parallel to the nanotube axis. The main observations are: (i) The dominant contribution to the splitting is independent of  $V_{\text{gate}}$ . (ii) As the field strength increases, the splitting is reduced (observed in all investigated cases) until only a single apparent peak remains. This field value is referred to as compensation field (here  $B_c \simeq 2$  T), since the dominant gate-independent part of the splitting is compensated. At higher fields the peak splits again. (iii) Despite (i), we observe nevertheless a slight gate dependence, in particular near  $B_c$ . This is most clearly reflected by the fact that the touching point of the two resonances moves from the left side of the CB diamond for  $B < B_c$  (cf.  $B = 1.5$  T) to the right side for  $B > B_c$  (cf.  $B = 2.5$  T). (iv) The gate dependence increases in strength very close to the edges of the CB diamond.

*Tunneling-induced level shifts.*— The presence of the splitting, its dependence on magnetic field, and a potential gate dependence can be consistently explained by the renormalization of the quantum dot level energy due to charge fluctuations between the dot and the leads. Since the density of states (DOS) in the FM contacts is spin dependent, the same is true for the charge fluctuations and the corresponding energy renormalization. Hence, the renormalization results in a spin splitting of the dot level  $\Delta\varepsilon \equiv \delta\varepsilon_\uparrow - \delta\varepsilon_\downarrow - g\mu_B B$ . For a single impurity Anderson model, the correction  $\delta\varepsilon_\sigma$  ( $\sigma = \uparrow, \downarrow$ ) from second order perturbation theory is (see, e.g., Ref. [10]):

$$\delta\varepsilon_\sigma \simeq -\frac{1}{\pi} \int d\omega \left( \frac{\Gamma_\sigma(\omega)[1-f(\omega)]}{\omega - \varepsilon_{d,\sigma}} + \frac{\Gamma_{-\sigma}(\omega)f(\omega)}{\varepsilon_{d,-\sigma} + U - \omega} \right). \quad (1)$$

Here,  $\varepsilon_{d,\sigma} = \varepsilon_d \mp g\mu_B B/2$  is the quantum level energy for spin  $\sigma$ ,  $U$  the charging energy, and  $\Gamma_\sigma(\omega)$  the spin-dependent tunneling rate.  $f(\omega)$  is the Fermi function.

From Eq. (1) one sees that the splitting is not only

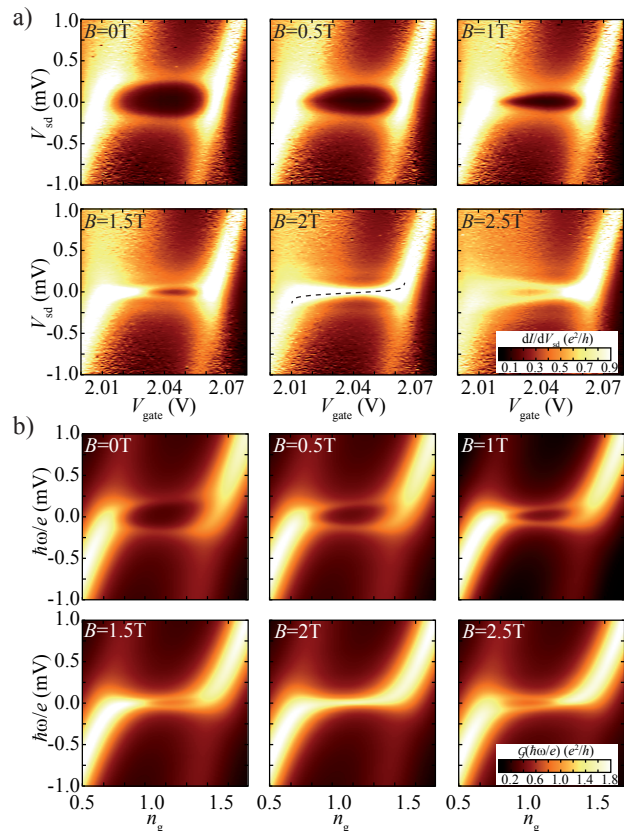


FIG. 2. (Color online) Differential conductance versus source-drain and gate voltage, in CB region 1 of Fig. 1, for six magnetic field values. We compare here (a) experimental data with (b) NRG results for the normalized zero-temperature spectral function  $\mathcal{G} = \sum_\sigma \pi \Gamma_\sigma(0) A_\sigma(\omega)$ , obtained using the model and parameters described in the text.  $n_g = 1/2 - \varepsilon_d/U$  is the dimensionless gate potential. The dashed line in the panel for  $B = 2$  T in (a) indicates the gate-dependent contribution from the polarization for  $\mathcal{P} = 10\%$  (see text).

a consequence of properties at the Fermi surface, but of the full DOS. The first and second terms in Eq. (1) describe electron- or hole-like processes, meaning fluctuations between the states  $|1, \sigma\rangle$  and  $|2\rangle$  or  $|0\rangle$ , respectively (the numeral denotes the charge occupation of the quantum dot). The spin dependent energy corrections  $\delta\varepsilon_\sigma$  are negative, as always in second order perturbation theory. Consequently, the spin direction that favors fluctuations more strongly will have lower renormalized energy.

*Effect of Magnetization.*— First we assume a shift between bands of equal and constant DOS for different spin directions,  $\rho_\uparrow = \rho_\downarrow = \rho_0$ , described by a constant Stoner splitting  $\Delta_{\text{St}}$ , see Fig. 3. The tunneling induced splitting  $\Delta\varepsilon^{(\mathcal{M})}$  due to  $\Delta_{\text{St}}$  is directly related to the saturation magnetization  $\mathcal{M} \equiv (n_\uparrow - n_\downarrow)/N_a = \Delta_{\text{St}}/(2D_0)$ . Here  $n_\sigma = \rho_0(D_0 + \varepsilon_F \pm \Delta_{\text{St}}/2)$  is the number of spin- $\sigma$  electrons,  $\varepsilon_F$  the Fermi energy, and  $N_a$  the number of states per atom and spin. Starting from Eq. (1) we can deduce the spin orientation of the dot ground state as follows: Figs. 3(b) and (c) show the phase space available (hatched) for quantum charge fluctuations for a spin up

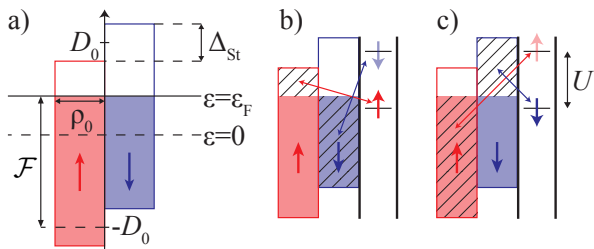


FIG. 3. (Color online) Schematic of the level renormalization process. (a) We assume flat bands  $\rho_\sigma(\omega) = \rho_0$  with bandwidth  $D_0$ , shifted with respect to each other by a constant Stoner splitting  $\Delta_{St}$ . The filling fraction  $\mathcal{F}$  determines the Fermi energy  $\varepsilon_F$ . (b) Charge fluctuations for a spin up electron on the dot, involving the empty states of the spin up band and the occupied states of the spin down band (hatched areas). (c) Analogous situation for a spin down electron on the dot; the available phase space (hatched) is larger than in (b).

or a spin down electron residing on the quantum dot, respectively. Comparing the total sizes of hatched areas for (b) and (c), the phase space is larger for the latter, thus favoring spin down. Therefore,  $\Delta\varepsilon^{(\mathcal{M})}$  is always negative, meaning that the energy correction due to a finite Stoner splitting is larger for the minority spin, i.e. the ground state spin is oriented opposite to the magnetization of the leads. This explains why the splitting is always initially reduced (never increased) when an external field is applied (cf. observation (ii) listed above; the magnetization direction follows that of the field in our setup). The size of this effect depends on the Stoner splitting, i.e., on  $\mathcal{M}$ . For  $|\varepsilon_d|, \varepsilon_d + U \ll D_0, \Delta_{St}$ , which is compatible with the experiment, we obtain, in extension of [11],

$$\Delta\varepsilon^{(\mathcal{M})} \simeq \frac{\Gamma}{2\pi} \ln \left[ \frac{(1 - \mathcal{M})^2 - (2\mathcal{F} - 1)^2}{(1 + \mathcal{M})^2 - (2\mathcal{F} - 1)^2} \right], \quad (2)$$

where  $\mathcal{F} = (1 + \varepsilon_F/D_0)/2$  is the filling fraction of the band. This shift is independent of the gate voltage (explaining observation (i)) because the position  $\varepsilon_d$  of the level is very close to  $\varepsilon_F$ , while the integration in Eq. (1) ranges over a large fraction of the d-band.

SQUID measurements allow us to determine a magnetic moment of  $\mu = 0.58 \mu_B/\text{atom}$  for our PdNi alloy [17], implying an effective magnetization of  $\mathcal{M} = 0.116$ . Ab-initio calculations of the band structure provide a filling fraction of  $\mathcal{F} = 0.853$  [18]. Thus, we estimate  $\Delta\varepsilon^{(\mathcal{M})} \simeq -175 \mu\text{eV}$ . In transport spectroscopy this would lead to conductance peaks split at zero external field by  $2\Delta\varepsilon^{\text{theo}}/e = 2|\Delta\varepsilon^{(\mathcal{M})}|/e \simeq 350 \mu\text{V}$ . Given the simplicity of our model, this agrees reasonably well with the experimentally determined peak distance of  $2\Delta\varepsilon^{\text{exp}}/e \simeq 550 \mu\text{V}$ . For a more weakly coupled resonance the predicted peak distance of  $60 \mu\text{V}$  agrees similarly with the experimentally found value of  $105 \mu\text{V}$ .

*Effect of polarization.*— The case of  $\rho_\uparrow \neq \rho_\downarrow$ , implying nonzero polarization  $\mathcal{P} = (\rho_\uparrow - \rho_\downarrow)/(\rho_\uparrow + \rho_\downarrow)$  at  $\varepsilon_F$ , has already been discussed in Refs. [6, 11] and earlier publica-

tions referenced there. Assuming a flat band with a spin-dependent DOS, e.g.  $\rho_\uparrow > \rho_\downarrow$  but zero  $\mathcal{M}$  for simplicity, quantum charge fluctuations renormalize the quantum dot level depending on its position relative to  $\varepsilon_F$ . This contribution shows a logarithmic divergence for  $\varepsilon_d \rightarrow 0$  and  $\varepsilon_d + U \rightarrow 0$  [6, 11], resulting in the up- and downward bending of the compensated conductance peak towards the corners of the diamond (cf. observation (iv)).

*Numerical results.*— The quality of our model is reflected by the close correspondence of Figs. 2(a) and (b). Fig. 2(b) presents high-quality NRG results for the spectral function  $A(\omega)$  [19] versus the normalized gate voltage  $n_g$ , calculated for a single-lead Anderson model with the DOS shown in Fig. 3 but with  $\rho_\uparrow \neq \rho_\downarrow$ , using *full* density-matrix NRG [20, 21]. Using the measured parameters of the quantum dot and modeling the ferromagnetism in the leads by taking  $\mathcal{P} = 10\%$  and  $\mathcal{M} = 0.116$ , very good agreement with experiment is found, except for the background current at high  $V_{sd}$ , which results probably from cotunneling processes involving higher levels not included into the model. In the experiment as well as in the numerical data, at  $B = 2 \text{ T}$  the gate-independent contribution, cf. Eq. (2), is fully compensated and the crossing point of the resonances lies in the center of the CB diamond. Here, only the (weak) gate-dependent contribution from  $\mathcal{P}$  remains (cf. observation (iii)), indicated in Fig. 2 ( $B = 2 \text{ T}$ ) by a dashed line. By varying  $\mathcal{P}$  and comparing the shape of the conductance peak at  $B_c$  between experiment and theory, we estimate  $\mathcal{P} \simeq 10\%$ .

*Universality.*— For a quantum dot coupled to normal leads, the normalized zero-bias conductance is a universal function (1) of  $\tilde{T} = T/T_K$  at zero field, and (2) of  $\tilde{B} = g\mu_B B/k_B T_K$  at zero temperature. (We define the Kondo temperature  $T_K$  via  $G(T = T_K)/G(0) = 1/2$  at zero field). We find, quite remarkably, that both these universal features are recovered also for ferromagnetic leads, if  $B$  is replaced by the effective field  $\delta B = B - B_c$ . Regarding (1), Fig. 4(d) shows that at the compensation field,  $B = B_c$ , the temperature dependence of the normalized conductance,  $G(T)/G(0)$ , agrees with the often-used semi-empirical formula  $\tilde{g}(\tilde{T}) = [1 + (2^{1/s} - 1)\tilde{T}^2]^{-s}$ , with  $s \simeq 0.22$  [3]. Although the latter behavior is well-established for dots coupled to normal leads, its emergence here is nontrivial: it demonstrates that despite the ferromagnetic environment, local spin symmetry can indeed be fully restored by fine-tuning the field to  $B_c$ .

The magnetic field dependence (2) has so far attracted much less attention [22]. To explore it, Fig. 4(a)-(c) shows  $G(B)$  at fixed  $T \ll T_K$  for several charge states differing in  $T_K$ ,  $B_c$ , and  $\Delta\varepsilon(B = 0)$ . The position of the conductance peak roughly follows the Zeeman law, with slight deviations in the vicinity of the compensation field  $B_c$  [22]. We find that  $B_c$  and  $T_K$  vary independently for different charge states, implying different couplings  $\Gamma$ .

According to (2),  $G(B)/G(B_c)$  should be a universal function of  $\delta\tilde{B} = g\mu_B(B - B_c)/k_B T_K$ . The lines

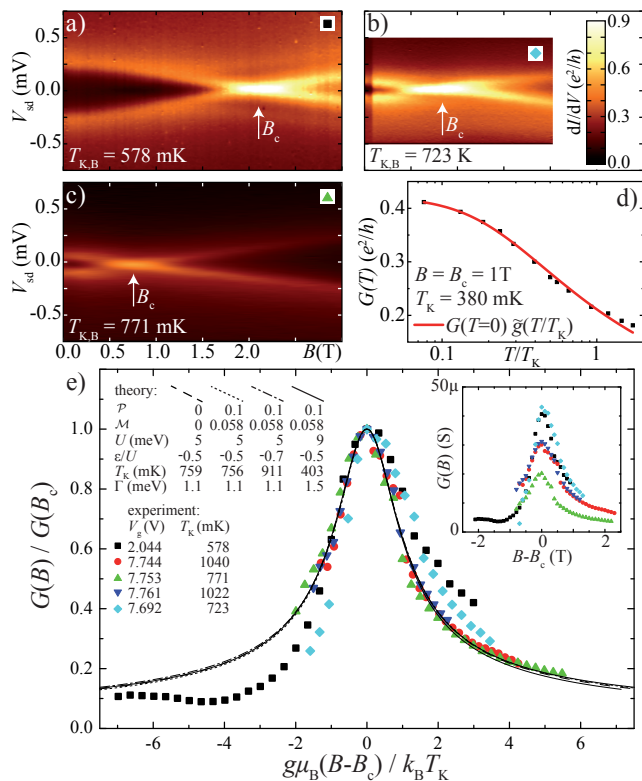


FIG. 4. (Color online) (a)-(c) Magnetic field dependence of the splitting for different charge states. Vertical arrows denote the compensation field  $B_c$ . (d) Scaling plot of  $G(T)$  vs.  $T/T_K$  (symbols), at  $B = B_c$ , for the charge state shown in Fig. 4(c); the solid line gives  $G(0)$  times the universal function  $\tilde{g}(T/T_K)$  discussed in the main text. (e) Scaled zero bias conductance  $G(B)/G(B_c)$  plotted against the effective normalized field  $\delta\tilde{B}$ , at fixed  $T = 50$  mK  $\ll T_K$  (100 mK for ■). Lines represent NRG calculations for several parameter sets. Inset:  $G(B)$  vs.  $(B - B_c)$  before scaling.

in Fig. 4(e) show this curve, calculated by NRG for four different sets of model parameters, yielding a good scaling collapse. Symbols show experimental data for  $G(B)/G(B_c)$  vs.  $\delta\tilde{B}$ , for several different gate voltages, with  $T_K$  extracted by numerical fitting to the NRG results. For three data sets taken on the same charge state (circles and triangles), scaling works very well and agreement with theory is excellent; for the other two sets (squares, diamonds), the quality of scaling is reduced at higher  $\delta\tilde{B}$  by an asymmetric background contribution to the magnetoconductance. Nevertheless, the overall agreement between theory and experiment shows that the model correctly captures the universal, sample-independent features of  $G(B)$  as function of  $\delta\tilde{B}$ .

*Conclusions.*— We have performed a quantitative comparison of the conductance of quantum dots with FM contacts, in the Kondo regime, with model NRG calculations. The quantitative agreement between experimental and numerical data lends strong support to the scenario proposed in Refs. 8 and 11: the exchange field induced by magnetic contacts causes the local level to be split

by an amount  $\Delta\varepsilon$ , which adds a constant offset to the Zeeman splitting induced by an external magnetic field. When this offset is compensated by a suitably fine-tuned field  $B_c$ , universal scaling features of the Kondo effect are recovered. The control of  $\Delta\varepsilon(B)$  through the selection of materials with proper  $\mathcal{M}$  and  $\mathcal{P}$  (high or small  $\mathcal{M}$  optimize peak splitting or gate tunability, respectively) may prove useful for future applications in spintronics.

We acknowledge fruitful discussions with M. Grifoni, S. Koller, J. Paaske, M. R. Wegewijs, and H. S. J. van der Zant, and thank S. Mankovsky for providing results of ab-initio calculations. This project has been supported by the DFG within SFB 689 and the NIM excellence cluster. I. W. was supported by the Polish MSHE and the Humboldt Foundation, and K. K. by the NRF of Korea under Grant No. 2009-0072595 and by the LG Yeonam Foundation. In the final stage of the preparation of this manuscript we became aware of a similar study in quantum dots with nonmagnetic contacts [23].

\* markus.gaass@physik.uni-regensburg.de

- [1] A. Hewson, *The Kondo Problem to Heavy Fermions* (Cambridge University Press, Cambridge, 1993).
- [2] I. Žutić, J. Fabian, and S. D. Sarma, *Rev. Mod. Phys.* **76**, 323 (2004).
- [3] D. Goldhaber-Gordon *et al.*, *Phys. Rev. Lett.* **81**, 5225 (1998).
- [4] S. M. Cronenwett, T. H. Oosterkamp, and L. P. Kouwenhoven, *Science* **281**, 540 (1998).
- [5] A. N. Pasupathy *et al.*, *Science* **306**, 86 (2004).
- [6] J. R. Hauptmann, J. Paaske, and P. E. Lindelof, *Nature Physics* **4**, 373 (2008).
- [7] L. Hofstetter *et al.*, *Phys. Rev. Lett.* **104**, 246804 (2010).
- [8] J. Martinek *et al.*, *Phys. Rev. Lett.* **91**, 127203 (2003).
- [9] M. S. Choi, D. Sánchez, and R. López, *Phys. Rev. Lett.* **92**, 056601 (2004).
- [10] J. Martinek *et al.*, *Phys. Rev. B* **72**, 121302 (2005).
- [11] M. Sindel *et al.*, *Phys. Rev. B* **76**, 045321 (2007).
- [12] J. Kong *et al.*, *Nature* **395**, 878 (1998).
- [13] S. Sahoo *et al.*, *Appl. Phys. Lett.* **86**, 112109 (2005).
- [14] L. P. Kouwenhoven *et al.*, in *Mesoscopic Electron Transport*, edited by L. L. Sohn, L. P. Kouwenhoven, and G. Schön (Kluwer, 1997).
- [15] Y. Oreg, K. Byczuk, and B. I. Halperin, *Phys. Rev. Lett.* **85**, 365 (2000).
- [16] S. Salmaz *et al.*, *Phys. Rev. B* **71**, 153402 (2005).
- [17] D. Steininger, A. K. Hüttl, D. Preusche, M. Ziola, M. Kiessling, M. Sperl, G. Bayreuther, and C. Strunk, in preparation (2011).
- [18] S. Mankovsky, private communication.
- [19] Though  $A(\omega)$  is calculated for an equilibrium model at zero temperature, its  $\omega$ -dependence mimics (qualitatively, if not quantitatively) the  $V_{sd}$ -dependence of the conductance for a two-lead setup.
- [20] A. Weichselbaum and J. von Delft, *Phys. Rev. Lett.* **99**, 076402 (2007).
- [21] We used the Budapest NRG code; O. Legeza *et al.*, arXiv:0809.3143, unpublished (2008).
- [22] C. Quay *et al.*, *Phys. Rev. B* **76**, 245311 (2007).
- [23] D. Goldhaber-Gordon *et al.*, unpublished (2011).